

Na²⁴ and P³² Formation

The Na²⁴ and P³² formed do not fall within the scope of the above discussion. Cross sections for their production are given in Table V. Because of the subtraction procedures involved in thick target bombardments, these cross sections are accurate to only $\pm 50\%$.

Energy requirements for the formation of these products are such that it is highly unlikely that they were formed by nucleon or alpha-particle emission. It therefore appears that heavy-ion-induced fission or fragmentation of medium-mass targets takes place with an appreciable cross section. Little more can be said on

the basis of present data, apart from the customary comment that it would be interesting to investigate this phenomenon further.

ACKNOWLEDGMENTS

The authors appreciate the help of the staff of the Yale Heavy Ion Accelerator for making this work possible. We are grateful to A. Friedman for help in finding thin aluminum catcher foils. Several discussions with J. Alexander and I. Preiss were most stimulating and helpful. This work was supported by the U. S. Atomic Energy Commission.

PHYSICAL REVIEW

VOLUME 127, NUMBER 5

SEPTEMBER 1, 1962

Excitation Functions of (p, xp) Reactions*

DAVID L. MORRISON†,‡ AND ALBERT A. CARETTO, JR.

Department of Chemistry, Carnegie Institute of Technology, Pittsburgh, Pennsylvania

(Received April 20, 1962)

Radiochemically measured excitation functions are reported for several (p, xp) reactions, where $x \geq 2$, for target nuclei encompassing a wide range of mass numbers and for incident energies of 100 to 440 MeV. The $(p, 2p)$ reactions were studied using Si³⁰, Zn⁶⁸, and W¹⁸⁶ as target nuclei; the $(p, 3p)$ reactions were studied using Si³⁰, P³¹, V⁵¹, As⁷⁵, W¹⁸⁶, and Re¹⁸⁷; the $(p, 4p)$ reactions were studied using P³¹, S³², As⁷⁵, and Re¹⁸⁷; and a $(p, 5p)$ excitation function was measured using S³² as the target. The data do not seem to exclude important contributions by either the knock-on or evaporation mechanisms in all mass regions studied, although, according to qualitative arguments it seems plausible that knock-on processes predominate in the high-mass region.

INTRODUCTION

NUCLEAR reactions by which both the mass and the charge of the target nucleus are reduced by $x-1$ units, where x is an integer, can be referred to as (p, xp) reactions. Only a few cross sections for $(p, 2p)$ reactions induced by 100 to 400 MeV protons have been reported,¹⁻⁵ and reported values of $(p, 3p)$ cross sections^{6,7} are even scarcer. Only one reported value of a $(p, 4p)$ cross section⁷ and none at all for $x \geq 5$ have been found.

A systematic study of (p, xp) reactions seems to be a logical step in trying to understand what happens

when a high-energy particle interacts with a complex nucleus. These reactions occupy the interval between simple reactions, which are beginning to be understood, at least qualitatively, and the spallation reactions in which the interactions are so complex as to defy all serious attempts at analysis or information extraction. In $(p, 2p)$ reactions only one of the target nucleons participates dominantly. As the value of x increases, the complexity of the problem increases in sufficiently small steps so that an understanding of the simpler reactions may help one to understand the more complex reactions if one studies such a sequence carefully. For those reactions in which only protons are emitted, there are fewer paths by which the product can be formed than in reactions where both proton and neutron emission must occur.

The general mechanism within which high-energy reactions have usually been interpreted was proposed by Heisenberg⁸ and by Serber,⁹ and is referred to in succeeding sections as the Serber process. According to this model, the high-energy reaction is roughly divided into two phases: (i) the knock-on cascade, in which a number of particles are ejected from the nucleus by direct interaction, leaving a residual

* Research performed under contract with the U. S. Atomic Energy Commission.

† Presented in partial fulfillment of the Ph.D. degree in the Department of Chemistry, Carnegie Institute of Technology, Pittsburgh, Pennsylvania.

‡ Present address: Battelle Memorial Institute, Columbus Ohio.

¹ J. M. Miller and J. Hudis, *Ann. Rev. Nuclear Sci.* **9**, 159 (1959).

² P. P. Strohal and A. A. Caretto, *Phys. Rev.* **121**, 1815 (1961).

³ W. R. Ware and E. O. Wiig, *Phys. Rev.* **122**, 1837 (1961).

⁴ D. W. Maurer, Ph.D. thesis, The University of Rochester, Rochester, New York, 1958 (unpublished).

⁵ A. A. Caretto and G. Friedlander, *Phys. Rev.* **110**, 1169 (1958).

⁶ G. Rudstam, Ph.D. thesis, University of Uppsala, Uppsala, Sweden, 1956 (unpublished).

⁷ J. B. Cumming, Atomic Energy Commission Report NYO-6141, 1954 (unpublished).

⁸ W. Heisenberg, *Naturwissenschaften* **25**, 749 (1937).

⁹ R. Serber, *Phys. Rev.* **72**, 1114 (1947).

TABLE I. Target materials.

Target nuclide	Abundance %	Form bombarded	Purity and supplier*
Si ³⁰	3.12	SiO ₂ powder	Spectroscopic—A
P ³¹	100	Amorphous red phosphorus	Spectroscopic—B
S (natural)		Crystalline powder	Spectroscopic—C
S ³²	95.0	Crystalline powder	Enriched to 97.90%—D
V ⁵¹	99.75	1-mil V metal foil	99.7% V—E
Zn ⁶⁸	18.56	Zn metal electroplated on 1-mil Au backing	Enriched to 96.8%—D
As ⁷⁵	100	As metal powder	Spectroscopic—A
W ¹⁸⁶	28.4	5-mil W metal sheet	Spectroscopic—F
Re ¹⁸⁷	62.93	1-mil Re metal sheet	Spectroscopic—G

* Suppliers are indicated as follows: A, Johnson, Matthey & Company, Ltd.; B, Fisher Scientific Company; C, American Smelting and Refining Company; D, Oak Ridge National Laboratory; E, Vanadium Corporation of America; F, General Electric Company; and G, J. A. Samuel and Company, Inc.

excited nucleus; (ii) the de-excitation of the residual excited nucleus through the emission of particles and photons, often called evaporation. Since the evaporation of protons is hindered by the Coulomb barrier, the knock-on cascade may be the predominating mechanism in (p, xp) reactions induced by high- Z targets.

Excitation functions have been measured on targets encompassing a wide range of mass numbers. The range of x covered was $2 \leq x \leq 5$, and incident proton energies were 100 to 400 MeV.

EXPERIMENTAL PROCEDURE

All irradiations were carried out in the circulating beam of the Carnegie Institute of Technology synchrocyclotron with proton energies of about 100 to

440 MeV. The length of bombardment was determined by the nature of the reaction being studied and the target material. Bombardment periods of 1 to 30 min were employed. The incident proton energy was varied by placing the target at different radial distances in the circulating beam. The uncertainty in the assignment of the proton energy due to the spread of proton energies in the beam, and to the variation of the nominal energy with magnetic field strength was estimated to be less than 10% at all energies.

All cross sections were measured relative to the cross section for the $\text{Al}^{27}(p, 3pn)\text{Na}^{24}$ monitor using 1-mil aluminum foil. The values of the monitor cross section used in this study were those of Hicks, Stevenson, and Nervik¹⁰ below 350 MeV and of Cumming, Friedlander, and Swartz¹¹ above 350 MeV.

The disintegration properties of the product nuclides, except for Ga^{73} and Hf^{184} , of the 14 nuclear reactions studied were taken from the compilation of Strominger, Hollander, and Seaborg.¹² The decay scheme for the Ga^{73} was reported by Goldemberg *et al.*,¹³ and for Hf^{184} by Merz.¹⁴ Table I contains a list of the elements bombarded, the form bombarded, and the purities and suppliers of the target materials. A detailed description of the methods of targeting can be found in the Appendix.

After bombardment the targets were dissolved in appropriate acids in the presence of carriers and adaptations of conventional radiochemical¹⁵ and analytical¹⁶ procedures were used for the purification of the products. The specific separation schemes

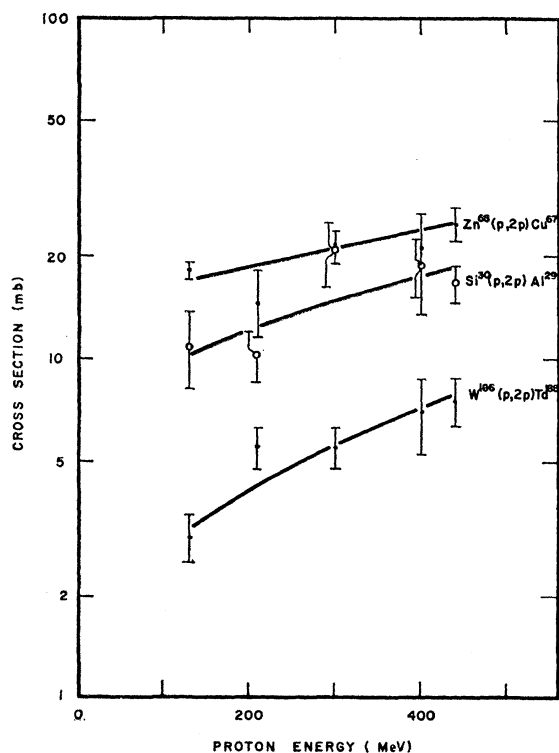


FIG. 1. Excitation functions for $(p, 2p)$ reactions.

¹⁰ H. G. Hicks, P. C. Stevenson, and W. E. Nervik, *Phys. Rev.* **102**, 1390 (1956).

¹¹ J. B. Cumming, G. Friedlander, and C. E. Swartz, *Phys. Rev.* **111**, 1386 (1958).

¹² D. Strominger, J. M. Hollander, and G. T. Seaborg, *Revs. Modern Phys.* **30**, 585 (1958).

¹³ J. Goldemberg, L. Marquez, E. W. Cybulski, N. L. Costa, and I. G. Almeida, *Nuclear Phys.* **10**, 28 (1959).

¹⁴ E. R. Merz (private communication).

¹⁵ W. W. Meinke, *Chemical Procedures Used in Bombardment Work at Berkeley*, Atomic Energy Commission Reports AECD-2738, 1949; AECD-2750, 1949; AECD-3084, 1951 (unpublished).

¹⁶ W. F. Hillebrand and G. E. F. Lundell, *Applied Inorganic Analysis*, revised by G. E. F. Lundell, H. A. Bright, and J. I. Hoffman (John Wiley & Sons, Inc., New York, 1953), 2nd ed.

TABLE II. Summary of experimental results.

Proton energy (MeV)	Average cross sections (mb)				
	130	210	300	400	425
Monitor					
$\text{Al}^{27}(p, 3pn)\text{Na}^{24}$	10.0	9.3	11.0	10.7	10.7
$\text{Si}^{30}(p, 2p)\text{Al}^{29}$	10.7 ± 2.8	10.2 ± 1.7	20.8 ± 4.6	18.6 ± 3.7	16.6 ± 1.9
$\text{Zn}^{68}(p, 2p)\text{Cu}^{67}$	18.1 ± 0.8	14.6 ± 3.3	21.3 ± 3.3	20.8 ± 5.8	24.8 ± 2.6
$\text{W}^{186}(p, 2p)\text{Ta}^{185}$	2.98 ± 0.48	5.55	5.48	6.93 ± 1.74	7.44 ± 1.21
$\text{Si}^{30}(p, 3p)\text{Mg}^{28}$	2.05 ± 0.46	1.71 ± 0.35	2.15 ± 0.35	2.80 ± 0.35	1.89 ± 0.08
$\text{P}^{31}(p, 3p)\text{Al}^{29}$	4.33 ± 0.72	6.70 ± 1.10	4.35 ± 0.80	8.13 ± 1.59	7.50 ± 1.03
$\text{V}^{51}(p, 3p)\text{Sc}^{49}$	0.158 ± 0.035	0.227 ± 0.037	0.472 ± 0.076	0.391 ± 0.048	0.640 ± 0.073
$\text{As}^{75}(p, 3p)\text{Ga}^{73}$	0.303 ± 0.087	0.394 ± 0.050	0.516 ± 0.038	0.582 ± 0.096	1.08 ± 0.14
$\text{W}^{186}(p, 3p)\text{Hf}^{184}$	0.243 ± 0.033	0.144 ± 0.001	0.295 ± 0.059	0.316 ± 0.065	0.319 ± 0.082
$\text{Re}^{187}(p, 3p)\text{Ta}^{185}$	$(3.85 \pm 1.35) \times 10^{-2}$	$(7.28 \pm 1.05) \times 10^{-2}$	8.51×10^{-2}	$(13.2 \pm 0.8) \times 10^{-2}$	$(9.65 \pm 1.46) \times 10^{-2}$
$\text{P}^{31}(p, 4p)\text{Mg}^{28}$	0.189 ± 0.022	0.207 ± 0.034	0.328 ± 0.065	0.277 ± 0.062	0.312 ± 0.030
$\text{S}(p, 4p)\text{Al}^{29}$	0.565 ± 0.141	0.414 ± 0.091	0.603 ± 0.070	0.529 ± 0.144	0.594 ± 0.071
$\text{S}^{32}(p, 4p)\text{Al}^{29}$	0.590			0.578	
$\text{As}^{75}(p, 4p)\text{Zn}^{72}$	$(2.60 \pm 1.74) \times 10^{-3}$	$(7.85 \pm 1.73) \times 10^{-3}$	$(8.53 \pm 1.72) \times 10^{-3}$	3.330×10^{-3}	
$\text{Re}^{187}(p, 4p)\text{Hf}^{184}$	$(4.88 \pm 0.20) \times 10^{-3}$	$(3.19 \pm 0.14) \times 10^{-3}$	$(3.80 \pm 0.87) \times 10^{-3}$	4.97×10^{-3}	
$\text{S}(p, 5p)\text{Mg}^{28}$	$(4.31 \pm 2.06) \times 10^{-3}$	$(5.48 \pm 0.82) \times 10^{-3}$	$(9.05 \pm 0.01) \times 10^{-3}$	$(4.60 \pm 1.04) \times 10^{-3}$	$(6.79 \pm 0.83) \times 10^{-3}$
$\text{S}^{32}(p, 5p)\text{Mg}^{28}$	4.71×10^{-3}			4.10×10^{-3}	

used may be found in Morrison's report.¹⁷ All the purified product activities were deposited as suitable precipitates on filter paper-disks using a glass-filter chimney. Chemical yields were all determined gravimetrically except for aluminum, which was determined spectrophotometrically.

The gross negatron activities were determined with end-window methane-flow β -proportional counters except for Mg^{28} which was counted with a Tracerlab TGC-2 Geiger-Müller tube. The aluminum monitor foils were counted in the same geometry as the corresponding product activities. A radium D-E source counted several times a week indicated a maximum change of 3% in the counting rate of the counters over the period of the measurements.

Absolute disintegration rates were determined for Na^{24} , Mg^{28} , and Cu^{67} by β - γ coincidence measurements. For the other product nuclides, counting efficiency factors were estimated by conventional methods. Air, detector window, and source cover absorption factors were calculated from the empirically determined formula of Gleason *et al.*¹⁸ Saturation back-scattering factors were taken from the work of Burt.¹⁹ The factors for self-absorption and self-scattering of the radiation by the source f_s were experimentally determined for the equilibrium mixture of Mg^{28} and Al^{28} . All other values for f_s were estimated from the curve of Nervik and Stevenson.²⁰

For Zn^{72} , Hf^{184} , and Ta^{185} , it proved convenient to count the radioactive daughter of the reaction product and thereby to avoid the resolution of complex decay

curves. Least-squares analyses of all decay curves, except for the copper and tungsten samples, was performed with a digital computer. The copper and tungsten decay curves were resolved graphically.

RESULTS

The experimentally determined values of the (p, xp) cross sections are given in Table II. The errors listed

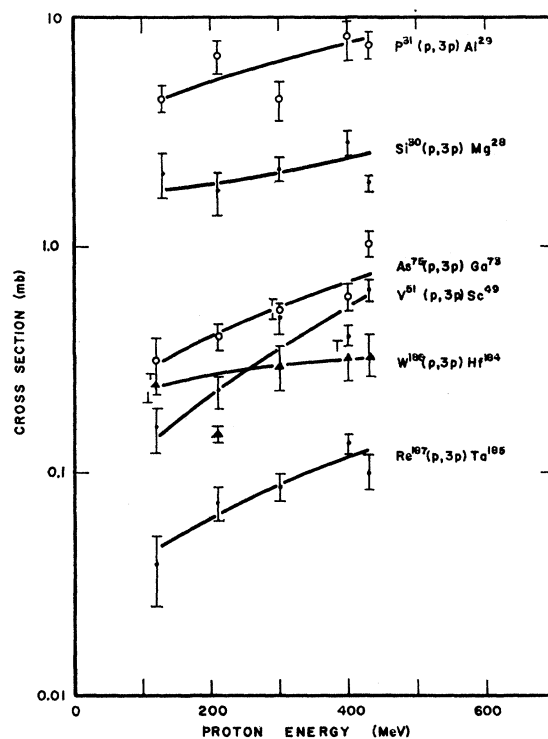


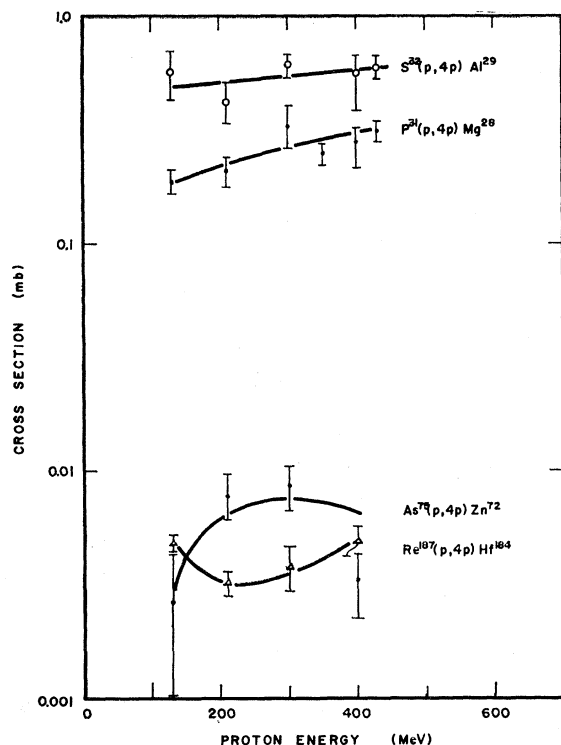
FIG. 2. Excitation functions for $(p, 3p)$ reactions.

¹⁷ D. L. Morrison, Atomic Energy Commission Report NYO-8921 (unpublished).

¹⁸ G. I. Gleason, J. D. Taylor, and D. L. Tabern, *Nucleonics* 8, 12 (1951).

¹⁹ B. P. Burt, *Nucleonics* 5, 28 (1949).

²⁰ W. E. Nervik and P. C. Stevenson, *Nucleonics* 10, 18 (1952).

FIG. 3. Excitation functions for $(p,4p)$ reactions.

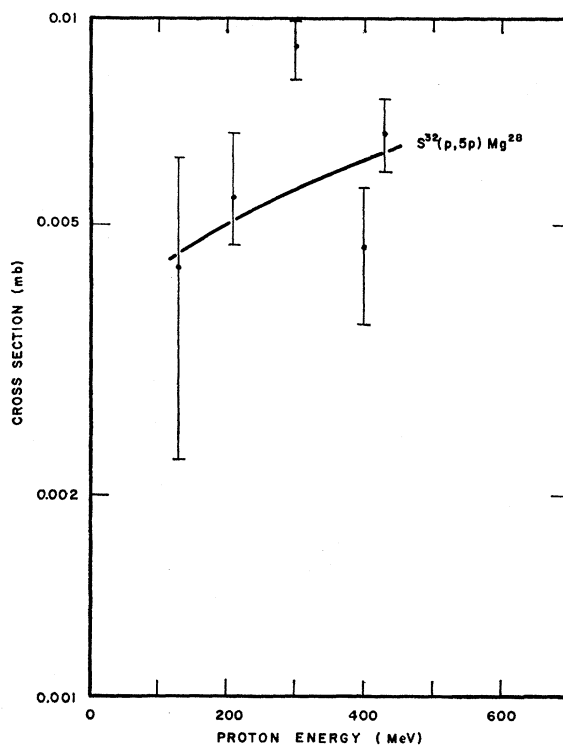
are for the standard deviation from the average for replicate determinations. Values with no cited uncertainties are single determinations. The excitation functions for the $(p,2p)$ reactions are plotted in Fig. 1, for the $(p,3p)$ reactions in Fig. 2, for the $(p,4p)$ reactions in Fig. 3, and for the $(p,5p)$ reaction in Fig. 4. The dependence of the (p,xp) cross section at 400 MeV upon target mass number is shown in Fig. 5. The dashed lines connect points representing the same reaction and are not a prediction of the functional dependence. The points at $A = 94$ and 142 are from the data of Strohal² and refer to the $Zr^{96}(p,2p)$ and $Ce^{142}(p,2p)$ reactions, respectively.

The value of the monitor absolute cross section is uncertain by about $\pm 10\%$. The uncertainty in the ratio of the absolute disintegration rate of the product to the absolute disintegration rate of the Na^{24} activity is less than $\pm 15\%$. The uncertainties in counting efficiency were ascertained by comparing the counting yield factors which were determined by the β - γ coincidence measurements with those that would be estimated for those nuclides. In addition to the counting yield uncertainties, the absolute disintegration rates may be affected by the decay curve resolution. This uncertainty is estimated to be $\pm 5\%$ for the activities resolved by the computer and about $\pm 10\%$ for samples resolved graphically. The error, which is taken to be the square root of the sum of the squares of the pertinent uncertainties, is $\pm 20\%$ for foil targets and $\pm 25\%$ for the powdered targets.

DISCUSSION

From the summaries of the experimental results presented in the preceding section, several significant features bear mention. For the $(p,2p)$ reactions, the general shape of the excitation functions and the magnitude of the cross sections are in agreement with other reported measurements in this energy region. The $(p,2p)$ and $(p,3p)$ excitation functions increase slightly with increasing energy, while the $(p,4p)$ excitation functions are nearly insensitive to bombarding energy. It is difficult to conclude the energy dependence of the $(p,5p)$ reaction due to the large experimental uncertainties.

There seems to be a different target mass number dependence at least for target nuclei with $A < 75$, for the $(p,2p)$ reaction than for the $(p,3p)$ and $(p,4p)$ reaction (see Fig. 5). This dependence is qualitatively repeated at all energies. The $(p,2p)$ cross section appears to be less sensitive to the mass number of the target, while the $(p,3p)$ and $(p,4p)$ cross sections generally decreased as the mass number of the target increased. An interesting behavior of the general mass number trend of the $(p,3p)$ and $(p,4p)$ reactions occurred in the Si^{30} , P^{31} , and S^{32} target series. At all energies the odd-mass-number product, Al^{29} , has a higher cross section than the even-even product Mg^{28} . A dependence on the odd-even mass number character of the product might be expected if the reactions proceed with a large evaporation contribution, so that

FIG. 4. Excitation function of the $S^{32}(p,5p)Mg^{28}$ reaction.

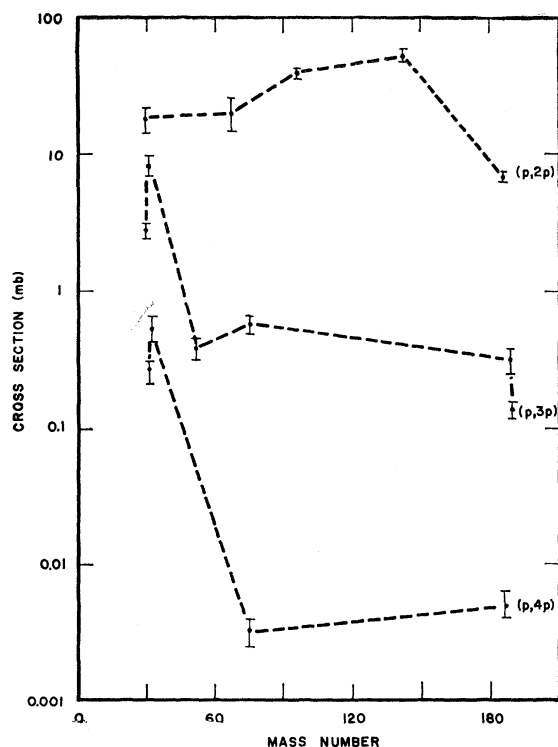


FIG. 5. Cross sections for (p, xp) reactions at 400 MeV vs mass number. (p, xp) points at $A=96$ and 142 are from reference 2.

the level densities and pairing energies of the product became important.

The values obtained for the $W^{186}(p, 2p)Ta^{185}$ reaction in this work are almost a factor of 10 lower than those reported by Strohal.² A third independent measurement of this cross section in this laboratory was carried out by Reuland²¹ and is in essential agreement with the value reported here.

Both steps of the Serber mechanism of nuclear reactions have been investigated in considerable detail by Monte Carlo methods.^{22,23} Application of the results of these studies to $(p, 2 \text{ nucleon})$ reactions has been made by several experimenters.^{3-5,24-27} In these cases, the energy dependence of the cross section has been reproduced reasonably well but the calculated values were too low by factors between 2 and 4. Very good agreement has been obtained by Ladenbauer and Winsberg,²⁵ between the calculated and measured values for the $I^{127}(p, pxn)$ cross sections at 160 and 450

MeV when x is greater than or equal to 2. Because $(p, 3p)$ reactions may be considered as (p, pxp) reactions, it might be expected that similar calculations would reproduce the experimentally measured values for the proton reactions as well.

The pure knock-on contribution to (p, xp) reactions was calculated from the cascade data of Metropolis *et al.*²² The Metropolis Monte Carlo calculations were based on a square-well Fermi gas potential and a rectangular mass distribution. A detailed discussion of these cross-section calculations may be found elsewhere.¹⁷ The results of these calculations are summarized in Table III. For the calculations of the $(p, 2p)$ and $(p, 3p)$ cross sections, cascade data for Al^{27} were used for comparison with the reactions on Si^{30} , P^{31} , and S^{32} ; data for cascades on Cu^{64} were used for V^{51} and As^{75} . Data on Bi^{209} were used for comparison with $W^{186}(p, 2p)Ta^{185}$ and to improve the statistical accuracy, were combined with Ce^{140} data for comparison with W^{186} and $Re^{187}(p, 3p)$ cross sections. For all $(p, 3p)$ cascades, the number of cases leading to excitation energies below particle evaporation thresholds was very small so that the final results should be used only as a guide to what might be expected from Monte Carlo treatments of this reaction mechanism if many more cases had been run. Out of 957 cascades on Al^{27} only (0.14 ± 0.37) cascades lead to $(p, 3p)$ products with an excitation energy equal to or less than the cutoff for particle evaporation. The situation is improved for Cu^{64} where, out of 964 cascades, (1.90 ± 1.38) $(p, 3p)$ cascades lead to products with proper excitation energies.

Although the contribution to the calculated cross section values by proton evaporation has been neglected it would appear that at least in the medium- and heavy-mass region, the magnitude of the calculated $(p, 2p)$ cross section is too low by about a factor of 1.3 to 4 except for the tungsten target. Probably the same dependence upon nuclear model is important here as is supposed in the (p, pn) case.²² The use of the rectangular mass distribution in the Monte Carlo calculations probably de-emphasized the number of successful low

TABLE III. Comparison of Monte Carlo cascade calculations and experimental cross sections at 300 MeV.

Reaction	Experimental (mb)	Calculated (mb)
$Si^{30}(p, 2p)Al^{29}$	20.8 ± 4.6	15.5 ± 2.9
$Zn^{68}(p, 2p)Cu^{67}$	21.3 ± 2.1	13.3 ± 3.7
$Ce^{142}(p, 2p)La^{141}$	47.6 ± 2.7^a	10.4 ± 3.1^a
$W^{186}(p, 2p)Ta^{185}$	5.5 ± 1.1	10.1 ± 3.6
$Si^{30}(p, 3p)Mg^{28}$	2.15 ± 0.24	0.075 ± 0.20
$P^{31}(p, 3p)Al^{29}$	4.35 ± 0.80	0.077 ± 0.20
$V^{51}(p, 3p)Sc^{49}$	0.472 ± 0.076	1.27 ± 1.03
$As^{75}(p, 3p)Ga^{73}$	0.516 ± 0.038	1.6 ± 1.3
$W^{186}(p, 3p)Hf^{184}$	0.316 ± 0.065	0.86 ± 1.34
$Re^{187}(p, 3p)Ta^{185}$	0.132 ± 0.080	0.86 ± 1.34

^a At 350 MeV, experimental reference 2, calculation reference 3.

²¹ D. Reuland (private communication).

²² N. Metropolis, R. Bivins, M. Storm, A. Turkevich, J. M. Miller, and G. Friedlander, *Phys. Rev.* **110**, 185 (1958); N. Metropolis, R. Bivins, M. Storm, J. M. Miller, G. Friedlander, and A. Turkevich, *ibid.* **110**, 204 (1958).

²³ I. Dostrovsky, Z. Fraenkel, and G. Friedlander, *Phys. Rev.* **116**, 683 (1959).

²⁴ H. R. Yule and A. Turkevich, *Phys. Rev.* **118**, 1591 (1960).

²⁵ I. Ladenbauer and L. Winsberg, *Phys. Rev.* **119**, 1368 (1960).

²⁶ S. S. Markowitz, F. S. Rowland, and G. Friedlander, *Phys. Rev.* **112**, 1295 (1958).

²⁷ N. T. Porile, *Phys. Rev.* **125**, 1379 (1962).

excitation ($p, 2$ nucleon) collisions. The similarity between (p, pn) and $(p, 2p)$ reaction cross sections in energy and mass number dependence, and the correspondingly similar behavior with regard to the low results from the Monte Carlo calculations may be an indication that the $(p, 2p)$ reaction proceeds with a large pure knock-on contribution. However, the extremely large uncertainties in the calculated values of $(p, 3p)$ cross sections from the Monte Carlo cascades does not allow one to make any kind of qualitative statement as to the cascade contribution to (p, xp) reactions when $x > 2$.

Although there are as yet no calculations adequate to guide the interpretation of these data, it is still interesting to see whether the increasing complexity of the (p, xp) reactions as x increases can be correlated in more than a qualitative way with the corresponding systematic decrease in the cross sections. An attempt at such a correlation is described below.²⁸

Assuming that the (p, xp) reactions proceed entirely by a knock-on mechanism, one tries to find ways (i) to express the reaction in separate x -dependent factors, (ii) to estimate the contributions of each factor, and then (iii) to combine the estimated contributions to obtain a plausible prediction for the (p, xp) cross sections relative to each other, for a given target (or given narrow region of target mass numbers). Since for even the simplest knock-on mechanism the geometrical details and energetics are almost intractably complicated, it is necessary to choose the relevant factors so that in simple and plausible ways they can account for the overall consequences of the much more complicated process. Accordingly, the estimate of relative (p, xp) cross sections is considered in terms of the following five factors, estimates for which are given with a rectangular mass distribution in mind:

1. The probability that the initial collision of the incident proton and all succeeding collisions are with protons within the nucleus. To a reasonable approximation, neglecting the effective cross sections for proton-nucleon collisions within the nucleus and the reduction in the number of available collision partners as the cascade proceeds, this factor is proportional to $(Z/A)^{x-1}$.

2. The cross section is proportional to some effective successful reaction volume. This volume has a cylindrically symmetric "shape," the diameter of which is roughly independent of x and proportional to the nuclear radius R , but the mean thickness of which should be of the order of the average mean free path of all the emergent protons, i.e., near

$$\frac{\bar{l}}{x\sqrt{x}} \propto \frac{1}{x} \left(\frac{1}{x} \right)^{\frac{1}{2}},$$

²⁸ This expression for the estimation of (p, xp) cross sections was developed during discussions between the authors and J. Robb Grover.

where \bar{l} is the mean free path of the incident proton, and assuming an inverse velocity dependence of the proton-nucleon cross section.

3. The relative probability that the incident particle reaches the reaction zone must be estimated. Assuming that the effective mean impact parameter for successful reactions is roughly independent of x , one obtains for this factor: $\exp[1/x\sqrt{x}]$.

4. The probability that the reaction which takes place in the reaction volume is $(p, x$ nucleon) rather than some other reaction, such as $(p, [x+1]$ nucleon), $(p, [x-1]$ nucleon), (p, p) etc. must be included. This factor is roughly proportional to

$$\prod_{j=1}^{x-1} \{1 - \exp[-(j/x)^{\frac{1}{2}}]\}.$$

5. Because only knock-on processes are considered, the residual nucleus from the cascade must be left with excitation less than that required for particle evaporation. Since these calculations are to be normalized to the $(p, 2p)$ cross section, this factor has the approximate form $[1/(x-1)!](\xi)^{x-2}$, where ξ is the fraction of the nuclear protons loosely enough bound that the "hole" resulting from the sudden removal of one of them will contribute less than 8-MeV excitation energy. For a simple Fermi gas $\xi \approx 0.4$.

The final expression for the (p, xp) cross section, from knock-on considerations only, is

$$\sigma_{p, xp} \propto \left(\frac{Z}{A} \right)^{x-1} \frac{1}{x\sqrt{x}} \times \exp\left(\frac{1}{x\sqrt{x}} \right) \prod_{j=1}^{x-1} \{1 - \exp[-(j/x)^{\frac{1}{2}}]\} \frac{1}{(x-1)!} (\xi)^{x-2}.$$

The above must not be considered the "derivation" of an expression for (p, xp) cross sections. It is only a plausible argument culminating in an expression capable of providing a first orientation to the behavior of (p, xp) cross sections as x is increased. Qualitatively, since every one of the five factors decreases with increasing x , one would predict that the cross sections should decrease rather steeply as x increases, as is actually observed.

The results of a calculation using this formula are presented in Fig. 6. The solid lines join the calculated values normalized to the experimental cross sections at 400 MeV for $\text{Si}^{30}(p, 2p)\text{Al}^{29}$ and $\text{W}^{186}(p, 2p)\text{Ta}^{185}$. The open circles are the experimental cross sections at 400 MeV for $A \sim 31$ and the solid circles are experimental cross sections for $A \sim 186$. As can be seen from Fig. 6, the calculated cross sections for the heavy-mass targets reproduce the steep decrease with increasing x as well as could be expected. However, in the light-mass region, the formula overestimates the rate of decrease. This might be interpreted as an indication

that evaporation processes are also important as a mechanism for the production of (p, xp) reaction products from light-mass targets. Similar observations were made for corresponding comparisons at the other energies.

A more compelling reason for invoking an important evaporation contribution to the reaction mechanism at the smaller mass numbers is that it can be used to explain the observed mass-number dependence of the ($p, 3p$) and ($p, 4p$) cross sections leading to Mg^{28} and Al^{29} . For example, at an excitation energy of 28 MeV, the ratio of the relative emission rates due to evaporation for protons from Si^{30} to that for protons from Al^{29} is 2.0. If a large part of the ($p, 3p$) and ($p, 4p$) reactions in this mass region proceed through evaporation and if the probability of forming Si^{30} by cascades from P^{31} and S^{32} is about the same as the probability of forming Al^{29} from Si^{30} and P^{31} respectively, then the experimentally observed ratios of

$$\sigma[\text{P}^{31}(p, 3p)\text{Al}^{29}]/\sigma[\text{Si}^{30}(p, 3p)\text{Mg}^{28}]$$

and

$$\sigma[\text{S}^{32}(p, 4p)\text{Al}^{29}]/\sigma[\text{P}^{31}(p, 4p)\text{Mg}^{28}]$$

should be about 2. See Table IV. However, in the case of the ($p, 3p$) reactions on W^{186} and Re^{187} the even-even product nucleus Hf^{184} has a larger cross section than the odd-even product Ta^{185} at all energies. Apparently

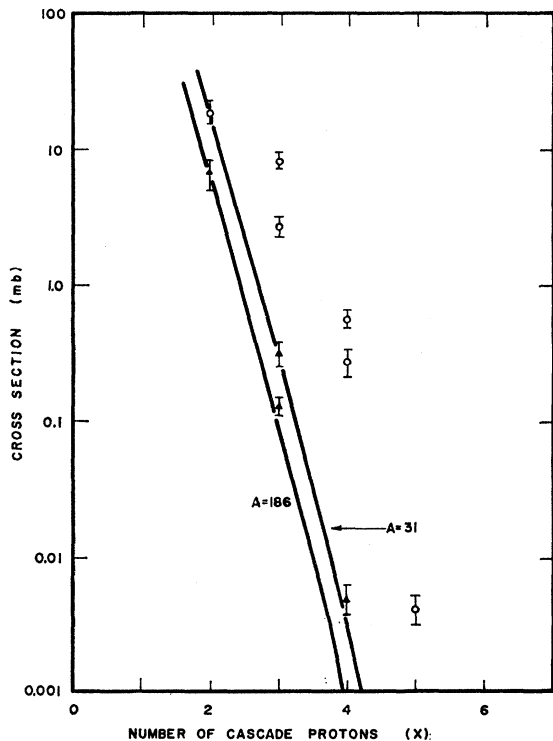


FIG. 6. Comparison of knock-on expression calculation with experimental data. Solid lines, calculation. Solid points, experimental data for $A \approx 186$. Open circles, experimental data for $A \approx 31$.

TABLE IV. Experimental cross-section ratios of $\text{Al}^{29}/\text{Mg}^{28}$ produced by ($p, 3p$) and ($p, 4p$) reactions compared with relative proton evaporation widths.

Proton energy (MeV)	130	200	300	400	425	Relative evaporation widths
$\text{P}^{31}(p, 3p)\text{Al}^{29}$						
$\text{Si}^{30}(p, 3p)\text{Mg}^{28}$	2.1	3.9	2.0	3.0	4.0	2.0
$\text{S}^{32}(p, 4p)\text{Al}^{29}$						
$\text{P}^{31}(p, 4p)\text{Mg}^{28}$	3.0	2.0	1.8	1.9	1.9	2.0

evaporation can not be as important with large- A targets otherwise similar behavior to the $\text{Al}^{29}/\text{Mg}^{28}$ ratio might be expected.

It has been shown by Kaufman²⁹ that it is reasonable to expect a sizeable contribution from a ($p, 3p$) cascade followed by one proton evaporation. He has shown that the production of Ga^{72} from As^{75} by ($p, 3pn$) can be accounted for if one assumes that a ($p, 3p$) cascade takes place followed by neutron evaporation to produce Ga^{72} and proton evaporation to produce Zn^{72} . On the basis of his calculation, Zn^{72} produced via evaporation paths accounted for approximately the total yield at 400 MeV. This is essentially in agreement with our calculation since the predicted cascade yield for a ($p, 4p$) reaction on As^{75} is about a factor of 8 lower than the experimental value.

APPENDIX

Two types of targets were used during the study. The foil targets were bombarded in a stack with an aluminum monitor foil. A square punch, 0.50 in. \times 0.50 in., was used to punch the target, guard, and monitor foils prior to bombardment. The areas obtained in this manner were quite reproducible, e.g., the several hundred aluminum foils punched out during this study weighed between 11.1 and 11.4 mg. By making a sharp fold in a piece of aluminum foil approximately 2 in. \times 1 in. \times 0.001 in., the target packet was formed. The leading edges of the foils were inserted into this fold in order to align the leading edges. The foils were stacked in such a manner that both the aluminum monitor and guard foils were upstream from the target, the aluminum guard foil between the target and the monitor. The edges of the outside foil were folded to hold the stack in place.

The oxide and powdered targets were bombarded in an aluminum dish packet. A Lucite die, 0.50 in. \times 0.50 in. \times 0.094 in., was used to form 1-mil aluminum foil dishes of corresponding sizes. A similar indentation was made in a 1-in. \times 2.50-in. \times 0.001-in. foil which served as the outside wrap of the target. The dish was placed in this indentation. A weighed amount of the target material was then placed in the dish, slurried

²⁹ S. Kaufman, Phys. Rev. **126**, 1189 (1962).

with acetone, and allowed to settle evenly on the bottom of the dish. This was covered with a few drops of Duco cement in acetone to hold it in place. An aluminum guard cap and aluminum monitor foil were placed in the dish on top of the target. The outside wrapper was folded over the top of this, leaving approximately a 0.125-in. lip protruding in front of the target. Targets were made by this technique of thicknesses from 10 to 60 mg cm⁻², depending upon the target nuclide.

Visual examination of the powdered targets indicated reasonably uniform target areas. The effect of a non-uniform target can be estimated by considering the beam distribution across the packet. An aluminum foil was cut into four equal strips parallel to the leading edge. A count of each piece gave the integrated Na²⁴ activity over that section. With this beam distribution, the total cross section for a given product was calculated as a function of the distribution of the powdered target

over the four sections. From visual estimates of the distribution of the powder in the most poorly made targets, the maximum error in the cross section was calculated to be $\pm 25\%$ compared to a uniformly distributed target. The estimated distribution of powder observed in most of the targets gave a calculated value for the error of $\pm 15\%$.

ACKNOWLEDGMENTS

We wish to thank Dr. J. Robb Grover for his suggestions and comments concerning the calculations based on the pure knock-on expression. The many helpful discussions and advice through all phases of this work by Professor Truman P. Kohman, Dr. Erich R. Merz, and Dr. John H. Gray are appreciated. The authors also wish to thank the operating staff of the Carnegie Institute of Technology Nuclear Research Center for their cooperation in carrying out the irradiations with the proton synchrocyclotron.